CYBERNETICS and COMPUTER TECHNOLOGIES

UDC 517.9:621.325.5:621.382.049.77 DOI:10.34229/2707-451X.23.1.7

M. KOSOVETS, L. TOVSTENKO

NEURAL NETWORK COMPONENT OF MODERN INFORMATION SYSTEM ON MOBILE PLATFORMS: LPI COGNITIVE RADAR SYSTEM

The problem of building modern systems for collecting, processing and presenting information for moving platforms, characterized by the presence of a neural network with deep learning, sensors with preprocessing, systems processing and presenting information, is considered. In modern systems the physics of the processes does not change, and accordingly, the algorithm for extracting signals from under the noise doesn't change either but is supplemented by a neural network that learns in the process of processing information to perform an applied task. Implementation example shown the introduction of artificial intelligence technology for the design a cognitive radar on a moving platform facilitates the transition from adaptive systems to cognitive ones.

***Keywords**: artificial Intellect, deep learning, neural network, cognitive radar, multiprocessor, Frequency modulation continuous wave, Radar Cross-Section, Solid State Transmitter.*

Introduction. Artificial intelligence has penetrated all the cracks of our life. Technical knowledge-intensive systems were not left aside either [1]. This includes medical systems, environmental monitoring systems, security systems, military systems, demining systems, monitoring in agriculture, and others. A special place is occupied by systems on moving platforms: drones, airplanes, helicopters, and others. Particular attention is paid to low-visibility systems, which are achieved by low radiation value, the use of sensitive signal receivers, the peculiarity of coding and transmission mode. All systems use Artificial Intelligence technologies to some extent: use of neural networks with learning, signal classification, image processing, etc. [2]. All components we consider through the prism of Artificial Intelligence have their own characteristics.

Let's consider the elements of a neural network component by component, ending with the training of the network and issuing the results in a form acceptable to the User. Let's start with the most common components of the network: receiving and transmitting radio wave components of the centimeter range, millimeter, terahertz, nano and *femto* range. Each wave range is interesting in its own way: it is the power, the presence of interference, the complexity of the reception-transmission path, the amount of information received, the conditions of use, etc., the cost of design and manufacture, the availability of specialists working with sensors are also taken into account. Modern Low Probability of Interception (*LPI*) radars are a class of radar systems that have certain performance characteristics that make them nearly invisible to modern intercept receivers [3–5]. The features of *LPI* radars include:

1) use of a narrow beam antenna with low side lobes;
2) transmitting radar pulses only when necessary;
3) reduction of transmitted pulse power;
4) spread of radar pulses in a wide band, so there will be only a very small signal on any one band; or use various transmission parameters such as: pulse shape, frequencies, or pulse repetition frequency (*PRF*) via intra-pulse modulation with imperceptible waveform.

The main characteristics of the transmission path:

- X-Band solid-state transmitter;
- Pulse compression and coherent processing;
- Variety of frequencies;
- Software – frequency management;
- Pulse Doppler processing;
- Low probability of intercept functions;
- Ability to choose peak power;
- Fully compatible with existing antennas.

The peculiarity of centimeter waves is the ability to spread over long distances, having small dimensions and weight. Having a radiation power of one watt, we can scan objects at a distance, for example, of up to 20 km. The very process of designing a network transceiver device is little different from the usual one, with the exception of the system for controlling the work of the receiving/transmitting path with a signal level below noise and cognitive capabilities. Interest is due to informativeness and relative simplicity of projection. They differ in frequency, sensitivity, power, modulation, amount of information, interface, object detection, etc.

Fig.1 shows a block diagram of a centimeter range radar system. It has typical radar reception and transmission units, reference generators, mixers, amplifiers, circulator, switches, signal limiters, analog-to-digital and digital-to-analog converters [6–10]. Construction THz radar will be discussed later.

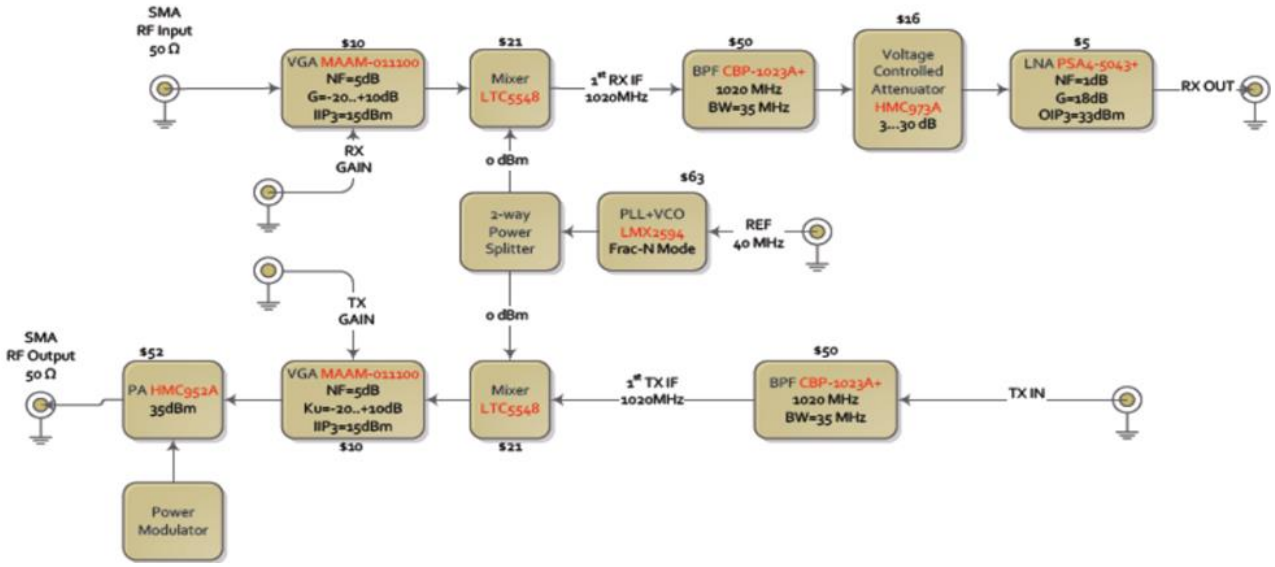

FIG. 1. Microwave board block diagram

This difference from similar radars lies in the regulation of qualitative characteristics not autonomously, due to feedback, but by the regulation of the cognitive abilities of the radar by the neural network [11, 12]. This article will introduce the construction of the radar, the characteristics of the reflected signals, the impact on them of interference and external and internal noise. This will allow deep learning tools to create a cognitive radar [13] with characteristics that are determined by the Customer.

1. Characteristics of reflected signals

Achieving the required characteristics of the radar largely depends on the frequency of the probed signals and the type of modulation [14]. The most frequently used ranges: m, cm, mm, THz. [14] Used types of modulation: [15] ultrawideband (UWB), frequency modulation continuous wave FMCW, [16, 17] pulse modulation, etc. Let's consider the most widespread pulse modulation. For radar with pulsed radiation, the signals reflected from a point target are a periodic sequence of bundles of pulses. The repetition period is equal to the antenna rotation time interval. The frequency of the sequence of pulses in the bundle is equal to the frequency of the sequence of probing pulses. The sequence of pulses Uc(t) in the bundle is modulated by the amplitude of the antenna directivity diagram G(t), expressed in time.

The directional diagram G(t) has a bell shape. Fig. 2 shows how the magnitude of the pulse power of the received signals changes over time due to the rotation of the antenna in the direction of the point object.

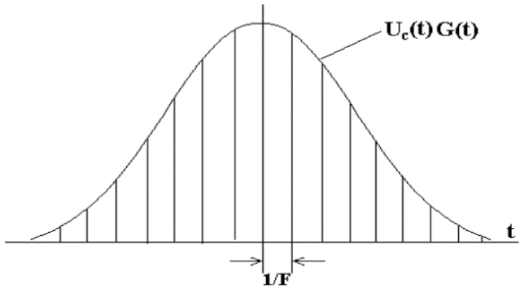

FIG. 2. The graph of the change in the value of the pulse power of the received signals over time due to the rotation of the antenna

With uniform rotation of the antenna, the number of pulses in a bundle

$$N = \alpha_H F / v_A, \tag{1}$$

where α_H (degrees) is the width of the antenna's horizontal directivity diagram;

F (Hz) is the sequence frequency of probing pulses;

v_A (degrees/s) is angular velocity of rotation of the antenna.

At an antenna rotation speed of 20 rpm, F = 1000 Hz, αH = 1°, is the number of pulses in a burst:

$$N = 1^{\circ} \frac{1000 Hz}{20 / 60 c^{-1}} = 8.3(3) \approx 8.$$

When the product is placed on a moving platform, the reflected pulses change in amplitude, resulting in a "friendly" fluctuation of pulses in the bundle.

The maximum range of radar detection depends on the technical parameters of the radar, the effective area of target scattering, the state of the atmosphere, the characteristics of the underlying surface, etc.

The minimum range of the radar is determined by the duration of the probing pulses, the recovery time of the receiver's sensitivity, including the inertia of the antenna switch when switching from the radiation mode to the reception mode.

The time interval τ_{pulse}, during which the probing pulse lasts, corresponds to the range

$$D(\tau_{pulse}) = \frac{c\tau_{pulse}}{2},$$

where c is the propagation speed of radio waves. If D [m], c [m/s], τ_{pulse} [μs], then we get D150 (τ_{pulse}).

At short ranges (less than 150 m), the pulse duration should be $\tau_{pulse} < 1 \mu s$. Then the minimum radar range will be obtained as:

$$D_{\min} \approx 300\tau_{pulse}.$$

It follows that to ensure $D_{\min} \approx 30\,\text{m}$, the pulse duration should be of the order of $\tau_{pulse} \approx 0.1\,\mu\text{s}$.

Range resolution is estimated by the distance ΔD between two separately observed targets 1 and 2, located in the same direction relative to the radar (fig. 3).

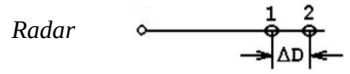

FIG. 3. The position of targets and radars when determining the resolving power by range

Separate reception of reflected signals from these targets is possible if the reflected pulse from the first target ends before the pulse reflected from the second target is received. Since the reflection from the first target lasts for the time τpulse, and the signal from the second target is delayed for the time $\Delta t = 2\Delta D/s$, the condition for separate reception of signals will be the inequality $\frac{2\Delta D}{c} \geq \tau_{pulse}$.

Separate display of two targets on the radar screen will be if the distance between the targets is:

$$\Delta D \geq \Delta D_{resolution} = c\tau_{pulse} / 2 . \quad (2)$$

As $\Delta D_{resolution}$ decreases, the range resolution increases. Thus, to increase the range resolution, the duration of the probing pulses should be reduced.

The azimuth resolution is estimated by the minimum value of the angle α_0 between the directions of two equidistant point targets 1 and 2 (fig. 4), at which the reflected signals from these targets are received separately.

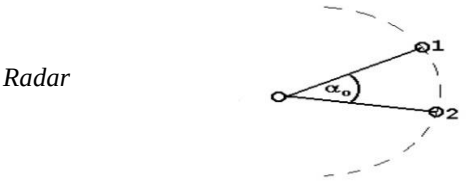

FIG. 4. Location of targets and radar when determining resolution along azimuth

The azimuth resolution α_0 is determined by the horizontal antenna beam width α_H at half power. Thus, to increase the resolution in azimuth, it is necessary to narrow the antenna pattern in azimuth.

The resolving area at distance D is estimated by the value of the area limited in azimuth by the beam width α_H of the antenna at half power, and in range by the range resolution (fig. 5). It should be noted that the range resolution due to the finite glancing angle β is 1/cosβ times greater than the generally accepted value $c\tau_{pulse} / 2$.

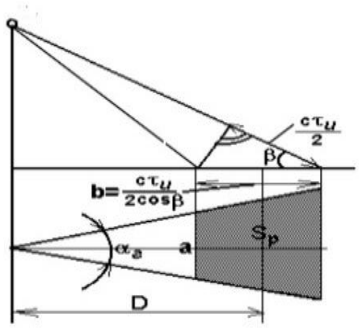

FIG. 5. Definition of resolving area

The slip angle is the angle in the vertical plane between the direction of maximum radiation from the output of the radar antenna and the ground surface.

The size of the resolving area:

$$S_{resolution} = \frac{D\alpha_H c\tau_{pulse}}{57.3 \cdot 2\cos\beta} = 0.0087\frac{D\alpha_H c\tau_{pulse}}{\cos\beta}.$$

For small values of β: $S_{resolution} = 0.0087 D\alpha_H c\tau_{pulse}$.

Calculation expression for resolving area

$$S_{resolution} = \frac{D\alpha_H 150 c\tau_{pulse}}{57.3} \approx 2.6 D\alpha_H \tau_{pulse} \text{ [m}^2\text{]}, \quad (3)$$

where α_H [degree]; τ_{pulse} [μs]; D [m].

Within the resolution area, point targets cannot be displayed separately on the Radar screen.

Else $D = 50 \cdot 10^3$ m $\alpha_H = 1°$; $\tau_{pulse} = 1$ μs, when $R_{resolutions} = 13 \cdot 10^4$ m^2.

The resolving volume at a distance D is estimated by the value of the volume, numerically equal to the cross-sectional area of the antenna beam at this distance, multiplied by the range resolution value (fig. 6), we get: $V_{resolution} = D^2 \frac{\alpha_H \theta}{(57.3)^2} \cdot \frac{c\tau_{pulse}}{2} = 1.5 \cdot 10^{-4} D^2 \alpha_H \theta c\tau_{pulse}$.

Calculation formula for resolving volume:

$$V_{resolution} = D^2 \frac{\alpha_H \theta}{(57.3)^2} \cdot 150\tau_{pulse} = 0.045 D^2 \alpha_H \theta \tau_{pulse}, \text{ [m}^3\text{]}, \quad (4)$$

where D[m]; α_H [degree]; θ [degree]; τ_{pulse} [μs].

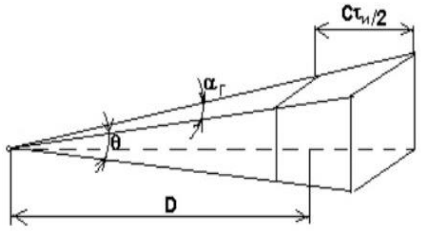

FIG. 6. Definition of resolving volume

2. Measurement error of navigation parameters

Let's consider the measurement errors of navigation parameters: distance to the target D_{tag}; azimuth to target α_{tag4}; target movement speed υ_{tag}.

The remaining parameters of the target are determined by calculation. The parameter measurement error depends on the instrumental and noise errors.

Instrumental errors in digital Radars depend on: the chosen interval of range measurement; the bit depth of the angle-code converter for measuring the angle of rotation of the antenna; the degree of optimality of the algorithms used for the operation of systems for detecting targets and measuring target parameters.

The resulting measurement errors depend primarily on: the impact of other radars; receiver's own noise level; hydrometeors, the effects of mutual interference.

Electromagnetic waves propagate in vacuum at a speed $c = \frac{1}{\sqrt{\mu_0 \varepsilon_0}} = 299792458 \approx 3 \cdot 10^8$ [m/s], where $\mu_0 = 4\pi \cdot 10^{-7}$ [H/m] – magnetic permeability, $\varepsilon_0 = \frac{1}{4\pi \cdot 9 \cdot 10^9}$ [F/m] – the dielectric constant.

For a medium with relative values of μ and ε, the energy propagation velocity is $v = \frac{c}{\sqrt{\mu\varepsilon}}$.

All types of the earth's surface are non-magnetic, therefore, for a surface wave, μ = 1. In the real Earth's atmosphere, the propagation velocity of radio waves υ is less than in free space, and depends on the refractive index *n*:

$$v = \frac{c}{\sqrt{\varepsilon}} = \frac{c}{n}, \tag{5}$$

where ε is the dielectric constant of the atmosphere, *c* = 299792458±1.2 m/s is the exact value of the propagation velocity of radio waves in vacuum.

The value of n is slightly greater than one, so:

$$v = \frac{c}{1 + \Delta n} \approx c(1 - \Delta n),$$

where $\Delta n = n - 1$ – refractive index.

In a real atmosphere, when determining the limiting distance, we take into account the refractive indices.

We give the dependence of the refractive index on the parameters of the atmosphere in the form of an empirical formula

$$(n-1) \cdot 10^2 \approx \frac{77.6}{T}\left(P_0 + P_1 + \frac{4810 P_1}{T}\right),$$

where *T* is the temperature [K], P_0, P_1 are the pressure of air and water vapor in megapascals.

In metrology 1 bar = 0.1 MPa = 760 mm *Hg*.

Experimentally, for a standard atmosphere, the average value of the refractive index was found:

$$(n-1) \cdot 10^6 \approx 313 \exp(-0.134H),$$

$$4\pi \frac{S^2}{\lambda^2} \cos^2 \alpha \left(\frac{\sin\left(\frac{2\pi a}{\lambda} \sin\alpha\right)}{\left(\frac{2\pi a}{\lambda} \sin\alpha\right)} \right)^2$$

where, α is the angle between the irradiation direction and the normal to the sheet;

- *a* is the horizontal length of the sheet;
- *S* is the leaf area.

For corner reflector, $4\pi \frac{a^4}{3\lambda^2}$ where a is the length of the edge side.

It can be seen from the formula that RCS, for all cases, is inversely proportional to the square of the wavelength λ. Corner reflectors are installed on weakly reflecting objects, increasing the range of their detection.

The table shows the experimentally obtained average values $\bar{S}_{RCS}$ for various types of targets with horizontal polarization of radio waves.

TABLE

Target type	Value (RCS) $\bar{S}_{RCS}$ [m^2]	Approximate calculation formula for (RCS) $\bar{S}_{RCS}$ [m^2]
Human	0,02 ... 0,05	-
Pillar	0,1 ... 0,2	-
Motorbike	3,0	$\bar{S}_{RCS} = ah^2$, where: a – coefficient, h – height Motorbike
A car	1,0 ... 5,0	-
Infantry fighting vehicles	50	-

The target RCS range is 60...70 db. Point targets at a close location of extended targets are difficult to detect. The range of RCS variation depending on the angle can vary by an order of magnitude.

The maximum target detection range essentially depends on the height of the radar antenna and the energy center of the target. The energy center of the target in height is the point at which the entire RCS is conditionally concentrated. The reflected signal from such a point is equal to the signal from the real target, distributed over the height.

During maneuvering, yaw and pitching of a moving target, the maximum values of impulses in a burst change in amplitude. There is a so-called "friendly" fluctuation of the amplitudes of the pulses in the pack.

3. Effective scattering surface

When the target moves, the geometry of the reflecting surface is constantly changing: part of the power of the probing signal is reflected from the target and enters the side of the radar, and part creates additional interference (clutter).

The reflected signals in this case are diffuse in nature, the probability distribution of instantaneous noise values has a normal distribution, the same as that of thermal noise.

We introduce the concept of the specific effective scattering surface $S_{sea,unit}$, which is equal to the ratio of the effective scattering surface S_{sea} to the resolving area $S_{resolution}$:

$$S_{sea,unit} = \frac{S_{sea}}{S_{resolution}},$$

where $S_{resolution}$ – resolving area, S_{sea} – effective scattering surface.

$$S_{sea} = S_{sea,unit} S_{resolution}. \quad (6)$$

The value of the specific effective scattering surface $S_{sea,unit}$ depends on the state of the surface, on the direction of irradiation relative to the direction of the wind, on the glancing angle β, on the range of waves, and on the type of polarization of electromagnetic waves. If the height of the Radar antenna above the

surface level is *h*, then the different glancing angles β correspond to the range *D*, which can be obtained from the expression

$$D = \frac{57.3h}{\beta},$$

where *h* [m]; *D* [м]; β [degree] for *h* = 30 m и β = 0,1°; 0,3°; 10°, then the corresponding range values *D* will be 17100; 5700; 1710 m.

For the case: distance $D \geq 17$ km; β = 0.1°; λ = 3 cm; horizontal polarization; surface state 5 points, – value $S_{sea,unit}$ = – 42 dB = 6.3 10−5.

If α_H = 1°; $\tau_и$ = 1 μs; *D* = 17000 m, then with expression (6) expression for resolving area:

$$S_{resolution} = \frac{D\alpha_H 150c\tau_{pulse}}{57.3} \approx 2.6D\alpha_H\tau_{pulse} \text{ [m}^2\text{]},$$

where α_H [degree]; τ_{pulse} [μs]; *D* [m], gives the value $S_{resolution}$ = 44200 m^2.

The effective scattering surface of hydrometeors (rain, snow, fog) is determined by the corresponding expressions:

$$S_{rain} = V_{resolution} \cdot V_{rain,unit},\ S_{snow} = V_{resolution} \cdot V_{snow,unit},\ S_{fog} = V_{resolution} \cdot V_{fog,unit},$$

where $V_{resolution}$ – resolution volume.

The values of specific RCS depend on the wavelength, plane of polarization, and intensity of hydrometeors. If λ = 3 cm, then the specific effective scattering surfaces for fog and rain are of the order of $V_{fog,unit} \approx 10^{-12}$ [1/m], $V_{rain,unit} \approx 10^{-5}$ [1/m].

At a distance *D* = 1000m, if α_H = 1 [degree]; θ = 20 [degree]; τ_{pulse} = 0,1 μs, then taking into account (6) calculation formula for the resolving volume

$$S_{rain} = V_{resolution} \cdot V_{rain,unit} \approx 0.045 \cdot 10^6 \cdot 20 \cdot 0.1 \cdot 10^{-5} \approx 0.90 \text{ m}^2.$$

Where *V*[m^3], *D* [м]; α_H [degree]; θ [degree]; τ_{pulse} [m]) effective rain scattering surface.

Against the background of the interfering effect of rain interference, it will be difficult to distinguish objects whose RCS is commensurate with the obtained value of 90 m^2, for example, boats, for which the RCS is 75 ... 250 m^2.

The specific RCS of hydrometeors decreases with increasing wavelength λ. So, for example, at a rain intensity of 100 mm/h for λ = 3 cm, the value of $V_{rain,unit} \approx 7 \cdot 10^{-5}$ [1/m], and for λ = 10 cm, is $V_{rain,unit} \approx 7 \cdot 10^{-7}$ [1/m], the specific RCS decreases by 2 orders of magnitude.

Multiple reflections from hydrometeors lead to additional noise at the input of the Radar receiver (weather clutter, volume clutter). The specific RCS of a thermal is 10^{-10} [1/m].

Frequency band: X-band 9200 — 9600 MHz (0.0326 — 0.0313 m); Peak Power: > 30 dBm (1 W).

For our 9-ft antenna, characteristics follows:

- Gain: ≥31 dB;
- Vertical beam width: 22 degrees +/−10%;
- Horizontal beam width: 0.85 degrees;
- Rotation speed: 22 rpm. +/−10%.

The antenna pattern is characterized Θ_A by the width of its main beam at a level of 0.5 of its maximum power value and the antenna gain G, which are related by the relations:

$$G = \frac{4\pi S_A}{\lambda^2},\ S_A = \frac{\pi d_A^2}{4},\ \Theta_A = \frac{\lambda}{d_A},$$

where S_A и d_A – effective area and length of the antenna aperture: Then $d_A = \frac{\lambda}{\Theta_A}$, $S_A = \frac{\pi d_A^2}{4} = \frac{\pi\lambda^2}{4\Theta_A^2}$, $G = \frac{4\pi S_A}{\lambda^2} = \frac{\pi^2}{\Theta_A^2}$.

In case the antenna beam width (in the horizontal plane)

$$\Theta_A = 0.85^\circ \cdot \frac{\pi}{180^\circ} = 0.014835 \text{ [rad], then}$$

$$d_A = \frac{\lambda}{\Theta_A} = \frac{c}{\Theta_A f_{ave}} = \frac{3\cdot 10^8}{0.014835\cdot 9.4\cdot 10^9} = 2.151 \text{ [m],}$$

$$S_A = \frac{\pi d_A^2}{4} = \frac{\pi\lambda^2}{4\Theta_A^2} = \frac{\pi c^2}{4 f_{ave}^2 \Theta_A^2} = \frac{\pi(3\cdot 10^8)^2}{4(9.4\cdot 10^9)^2\left(\frac{0.85\cdot\pi}{180}\right)^2} = 3.635 \text{ [m}^2\text{],}$$

$$G = \frac{4\pi S_A}{\lambda^2} = \frac{\pi^2}{\Theta_A^2} = \frac{180^2}{0.85^2} = 44844.290, \text{ what gives } G = 10\lg 44844.290 = 46.5 \text{ dB.}$$

Radar receiver input power: $P_r = S_A \cdot \rho_2 = S_A \frac{P_2}{4\pi R^2} = S_A \frac{\sigma\rho_1}{4\pi R^2} = S_A \sigma \frac{P_e}{(4\pi R^2)^2} G$, where ρ_2 is the power flux density of the wave of the given polarization reflected from the target at the point where the Radar is located; P_2 is the power reflected $P_2 = \sigma\cdot\rho_1$ by the target; σ – target RCS; ρ_1 is the power flux density of the incident wave of a given polarization at the target location; R – distance from the radar to the target; P_e is the power emitted by the Radar.

4. Range of radar observation of targets

The concept of "radar surveillance" includes a set of tasks: target detection; determination of coordinates; determination of target movement parameters.

The range of radar surveillance is determined by the power $P_{S,inp}$ of the reflected signals at the input of the receiver, which must not be less than the threshold value determined by the sensitivity of the receiver $P_{S,inp,\min}$.

When calculating the range of radar observation in free space, the following are not taken into account: attenuation of signals in the Earth's atmosphere under various weather conditions; the presence of additional interference due to re-reflections from hydrometeors, the properties of the underlying surface; the influence of two-beam propagation of radio waves, refraction, and so on.

Such a calculation of the range makes it possible to obtain only an approximate value of the real range of radar observation. If the Radar antenna is an isotropic radiator, then the radiated power flux is uniformly distributed over the surface of a sphere with a total area $4\pi D^2$, where D [m] is the distance from the Radar to the target. Power flux density W_{PFD} [W/ m^2] near the target

$$W_{PFD} = \frac{P_{pulse}\eta_{TX}}{4\pi D^2},$$

where P_{pulse} [W] – transmitter impulse power, η_{TX} – efficiency antenna-waveguide path of the transmitter.

The value $P_{pulse}\eta_{TX}$ represents the power of the emitted probing pulse. However, it should be taken into account that the real Radar antenna has high focusing properties, due to which the power flux density near the target increases significantly and amounts to

$$W_{PFD,1} = \frac{P_{pulse} G_A \eta_{TX}}{4\pi D^2},$$

where G_A is the directivity of the antenna.

Taking into account the absorption of a part of the incident power, the target re-radiates in the direction of the Radar power

$$P_1 = W_{PFD,1}\bar{S}_{tag} = \frac{P_{pulse} G_A \bar{S}_{tag} \eta_{TX}}{4\pi D^2},$$

where $\bar{S}_{tag}$ [m^2] – effective scattering surface of the target.

The power reflected from the target creates a power flux density near the radar antenna

$$W_{PFD,2} = \frac{P_1}{4\pi D^2} = \frac{P_{pulse} G_A \bar{S}_{tag} \eta_{TX}}{(4\pi)^2 D^4}.$$

At the output of the receiving antenna-waveguide path of the Radar (at the input of the receiver), we obtain the power

$$P_{S,inp} = W_{PFD,2} S_A \eta_{RX} = \frac{P_{pulse} G_A \bar{S}_{tag} S_A \eta_{TX} \eta_{RX}}{(4\pi)^2 D^4}, \quad (7)$$

where S_A [m^2] is the effective opening area (aperture) of the Radar antenna;

η_{RX} – efficiency receiving antenna-waveguide path.

There is a known relationship between the width of the antenna radiation pattern in the horizontal and vertical planes with the values of its aperture and wavelength in the form; $\alpha_H = \lambda / a$, $\theta = \lambda / b$, where λ [m] is the wavelength, α_H [rad], θ [rad] is the width of the antenna radiation pattern in the horizontal and vertical planes; *a* [m], *b* [m] are the dimensions of the antenna opening along the length and height.

Solid angle of the directional beam of the antenna:

$$\alpha_H \theta = \frac{\lambda^2}{ab} = \frac{\lambda^2}{S_A}.$$

The directivity of the antenna is calculated as the ratio of the solid angle of the sphere, equal to 4π, to the solid angle of the directional beam of the antenna

$$G_A = \frac{4\pi S_A}{\lambda^2}, \text{ where } S_A = \frac{G_A \lambda^2}{4\pi}. \quad (8)$$

With the help of (7) and taking into account the last relation (8), the power of the received reflected signals is equal to:

$$P_{S,inp} = \frac{P_{pulse} G_A^2 \bar{S}_{tag} \lambda^2 \eta_{TX} \eta_{RX}}{(4\pi)^3 D^4}.$$

If the received power at the receiver input $P_{S,inp}$ is taken equal to the receiver sensitivity $P_{S,inp,\min}$ (the minimum input signal level required to ensure the required quality of the received information), then the maximum range of radar surveillance will be represented as

$$D_{\max} = \sqrt[4]{\frac{P_{pulse} G_A^2 \overline{S}_{tag} \lambda^2 \eta_{TX} \eta_{RX}}{P_{S,inp,\min} (4\pi)^3}} . \quad (9)$$

The sensitivity of the radio receiver $P_{S,inp,\min}$ [W] is determined based on the following considerations.

The signal path of the receiver is a multi-stage device, which includes an input circuit, an RF amplifier, a mixer, and an intermediate frequency amplifier (fig. 1). In each cascade, the input noise $P_{N,inp}$ is amplified with a power and the own noise of this cascade is added with a power of $P_{N,add}$. As a result, a large noise power $P_{N,out} = P_{N,add} + P_{N,inp} G_{pwr}$ is observed at the output, where $G_{pwr} = P_{out} / P_{inp}$ is the power gain of the cascade. Using the noise floor power reduced to the input $P_{N,add,inp} = P_{N,add} / G_{pwr}$, we obtain a simple formula $P_{N,out} = (P_{N,add,inp} + P_{N,inp}) G_{pwr}$.

In order to quantify the inherent noise properties of each of the stages of the linear part of the receiver path, noise factor N_{factor} is used – a number showing how many times the signal-to-noise ratio in power SNR_{inp} at its input is greater than the corresponding ratio SNR_{out} at the output:

$$N_{factor} = \frac{SNR_{inp}}{SNR_{out}} = \frac{P_{S,inp} / P_{N,inp}}{P_{S,inp} G_{pwr} / (P_{N,add} + P_{N,inp} G_{pwr})} =$$
$$= \frac{P_{N,add} + P_{N,inp} G_{pwr}}{P_{N,inp} G_{pwr}} = 1 + \frac{P_{N,add}}{P_{N,inp} G_{pwr}} = 1 + \frac{P_{N,add,inp}}{P_{N,inp}}$$

where $P_{S,inp}$ – signal strength at the input.

The total noise figure is calculated by the formula (with cascades matched to each other)

$$N_{factor,\Sigma} = N_{factor,1} + (N_{factor,2} - 1) / G_{pwr,1} + (N_{factor,3} - 1) / G_{pwr,1} G_{pwr,2} + \ldots .$$

The source of external noise for the receiver is the antenna. The noise of the receiving antenna consists of the thermal noise of its active resistance and the noise of the radiation resistance due to the reception of radiation from space, the atmosphere, the Earth, as well as reflections from the underlying surface and hydrometeors. The overall noise of the antenna can be estimated by the mean square EMF of the noise from external radiation:

$$\overline{E}_{noise}^2 = 4 k T_A R_A \Delta f ,$$

where R_A is the radiation resistance of the antenna; T_A is the equivalent noise temperature of the antenna R_A, which makes noise like a real antenna, $T_A = T_{space} + T_{air} + T_{Earth}$, where T_{space}, T_{Earth}, are the noise temperature values associated with the penetration of cosmic noise, atmospheric noise and thermal radiation of the Earth into the antenna, respectively.

The power of external noise at the input of the receiver matched with the antenna (the internal resistance of the antenna as a signal source R_{gen} is equal to the input impedance of the receiver R_{inp}) will be $P_{N,inp} = k T_A \Delta f$.

The receiver noise floor power normalized to the input in the passband Δf [Hz] is estimated by the formula:

$$P_{N,add,inp} = P_{N,add} / G_{pwr} = kT_{RX}\Delta f = (N_{factor} - 1)kT_0\Delta f ,$$

where $k = 1.38 \cdot 10^{-23}$ [joule/K [degree]] constant Boltzmann's;

$T_{RX} = (N_{factor} - 1)T_0$ [K [degree]] – receiver equivalent noise temperature;

$T_0 = 293$ [K [degree]] (which corresponds 20 degree).

The total noise power at the output of the receiver (additional own and amplified external) is determined by the formula:

$$P_{N,out} = (P_{N,add,inp} + P_{N,inp})G_{pwr} = (kT_{RX}\Delta f + kT_A\Delta f)G_{pwr} = kT_0\Delta f G_{pwr}(t_{RX} + t_A),$$

where $t_A = T_A / T_0$ и $t_{RX} = T_{RX} / T_0$ – relative noise temperatures of the antenna and the amplifier path of the receiver.

The real sensitivity of the receiver is equal to the minimum signal power at the receiver input, at which the specified discrimination factor is provided. If at the output of the linear path of the receiver it is required to provide the signal-to-noise ratio $m = P_{S,out} / P_{N,out}$, then the required signal power at the input of the receiver $P_{S,inp,m} = mP_{N,out} / G_{pwr} = mkT_0\Delta f(t_{RX} + t_A)$ given that $t_{RX} = T_{RX} / T_0 = N_{factor} - 1$, and receive $t_A = T_A / T_0 = 1$, receiver sensitivity is real

$$P_{S,inp,\min} = P_{S,inp,m} = mN_{factor}kT_0\Delta f , \text{ [W]}. \quad (9)$$

When equality is fulfilled $P_{S,inp} = P_{S,inp,\min}$, the signal-to-noise ratio $q^2 = SNR_{out}$ (in terms of power) at the output of the receiver is equal to m. For reliable operation of radar surveillance systems, the value of *m* is chosen to be greater than one (in the case of using complex signals and matched filtering in the receiver, the value of m can be chosen to be less than one).

It is known that for a bell-shaped radio pulse with a duration τ_{pulse}, the optimal bandwidth Δf of a filter with a bell-shaped frequency response (the readings of the duration and bandwidth are taken at the level of 0.46) is determined from the relation $\Delta f = 1/\tau_{pulse}$. For a rectangular pulse with duration τ_{pulse}, the optimal bandwidth of a filter with a rectangular frequency response is $\Delta f = 1.37/\tau_{pulse}$.

In the future, we will assume that $\Delta f = 1/\tau_{pulse}$, the final expression for the range of radar observation will be presented in the form of an expression, which is called the "Basic equation of radar":

$$D_{\max} = \sqrt[4]{\frac{P_{pulse}G_A^2\tau_{pulse}\bar{S}_{tag}\lambda^2\eta_{TX}\eta_{RX}}{N_{factor}mkT_0(4\pi)^3}} . \quad (10)$$

It follows from expression (10) that in order to increase the range, $D_{\max}$ is advisable to increase G_A and λ as well.

The required value of the distinguishability coefficient m depends on the architecture of the receiver, the required probabilities of detecting and missing targets, and the errors in measuring the parameters of the movement of targets.

Radars on a moving platform emit a periodic sequence of single pulses. When reviewing point objects, the reflected signal is a burst of *N* pulses, so the signal-to-noise ratio (in terms of power) when processing not a single pulse, but a burst of pulses increases *N* times.

The probing signal when using this expression can be of any form: in the form of packets of phase-shift keyed pulses, parcels with linear frequency modulation, etc. In the simplest case we are considering, when a sequence of single pulses is emitted $\Delta f \tau_{pulse} = 1$, and the quantity $B = \tau_{pulse}$.

Conclusion

As a result of researching the market of modern radars, it was concluded that they have moved from purely special products to the social sphere. The parameters of the radar have also changed: invisibility, low radiation power, low probability of errors, wide range, use of different frequencies of the wave spectrum. In order to link consumer properties with quality characteristics, a trained neural network is needed to adjust the radar parameters. This makes it possible to model a radar with the dependence of qualitative characteristics on the hardware and software part even before manufacturing. Modularity will make it easier to get a radar with optimal price/quality indicators. Requirements for the design of transceiver modules are increasing, developments in IoT, cloud computing, and private cloud computing are used for special purpose radars.

The segment of radar technologies on mobile platforms is developing the fastest. Interest in them is due to the possibility of remote sensing of various objects, the territory: searching for mines, video recording, obtaining radar images, using the properties of the anisotropy of radar radiation, refraction, etc. Modern radars on mobile platforms are becoming cognitive, such a requirement is relevant for projects when others should not feel their presence.

References

1. Barkat M.On adaptive cell-averaging CFAR radar signal detection. Electrical Engineering and Computer Science. Dissertations. 1987. 276. https://surface.syr.edu/eecs_etd/276 (accessed: 20.04.2023)
2. Kosovets M., Tovstenko L. The Practical aspect of using the Artificial Intellectual Technology for building a multidimensional function CFAR for smart-handled LPI Radar. *Problem of Programming*. 2020. No. 2–3. UkrPROG'2020. 16-17 Sept. 2020. Kyiv, Ukraine. P. 304–312. http://dspace.nbuv.gov.ua/handle/123456789/180476
3. Han X., Chen S. Open-Set Recognition of LPI Radar Signals Based on Deep Class Probability Output Network. 2022. IEEE 8th International Conference on Computer and Communications (ICCC). 2022. Publisher: IEEE. https://doi.org/10.1109/ICCC56324.2022.10065669
4. Avdeyenko G., Narytnik T. Design of the Short-range FMCW Radar of the Terahertz Band. 2021 IEEE International Conference on Information and Telecommunication Technologies and Radio Electronics (UkrMiCo). 2021. IEEE. https://doi.org/10.1109/UkrMiCo52950.2021.9716617
5. Ren Z., Xiong Y., Li S., Wang D., Peng Z. Sub-Sampled Two-Dimensional SAR Imaging Method Based on MIMO FMCW Radar. 2020 International Conference on Sensing, Measurement & Data Analytics in the era of Artificial Intelligence (ICSMD). 2020. IEEE. https://doi.org/10.1109/ICSMD50554.2020.9261629
6. Deiana D., Suijker E.M., Bolt R.J., Maas A.P.M., Vlothuizen W.J., Kossen A.S. Real time indoor presence detection with a novel radar on a chip. 2014 International Radar Conference. IEEE. https://doi.org/10.1109/RADAR.2014.7060375
7. Wei G., Zhou Y., Wu S. Detection and localization of high speed moving targets using a short-range UWB impulse radar. 2008. IEEE. Radar Conference. IEEE. https://doi.org/10.1109/RADAR.2008.4720766
8. Liang Y., Liang X., He Y., Han W., Ge S. A novel ground moving target parameters estimation method for FMCW SAR. 2016 CIE International Conference on Radar (RADAR). IEEE. https://doi.org/10.1109/RADAR.2016.8059541
9. Giusti E., Martorella M. Range Doppler and image autofocusing for FMCW Inverse Synthetic Aperture Radar. 2009. International Radar Conference "*Surveillance for a Safer World*" (RADAR 2009). IEEE. https://ieeexplore.ieee.org/document/5438485

10. Shi S., Wang Y., Wang F., Zhou J. LPI Performance Optimization Scheme for a Joint Radar-Communications System. 2020 IEEE 11th Sensor Array and Multichannel Signal Processing Workshop (SAM). https://doi.org/10.1109/SAM48682.2020.9104362
11. Vakili M., Khosrojerdi S., Aghajannezhad P., Yahyaei M. A hybrid artificial neural network-genetic algorithm modeling approach for viscosity estimation of graphene nanoplatelets nanofluid using experimental data. Int. Commun. Heat Mass Transf. 2017. No. 82. P. 40–48. http://dx.doi.org/10.1016/j.icheatmasstransfer.2017.02.003
12. Kosovets M., Tovstenko L. Development of cognitive Radar Architecture. *Problem of Programming*. 2022. No. 1. P. 63–75. http://dspace.nbuv.gov.ua/handle/123456789/186204
13. Rudys S., Laučys A., Udris D., Pomarnacki R., Bručas D. Functionality Investigation of the UAV Arranged FMCW Solid-State Marine Radar. *J. Mar. Sci. Eng*. 2021. **9** (8). 887; https://doi.org/10.3390/jmse9080887
14. Kosovets M., Tovstenko L. Terahertz Radar of Image to study the Properties of Materials. *Journal «Zvjazok»*. 2018. No. 3. P. 40–46. http://con.dut.edu.ua/index.php/communication/issue/view/116
15. Park D.H., Bang J.H., Park J.H., Kim H.N. A Fast and Accurate Convolutional Neural Network for LPI Radar Waveform Recognition. 2022. 19th European Radar Conference (EuRAD). https://doi.org/10.23919/EuRAD54643.2022.9924721
16. Plata S., Wawruch R. CRM-203 Type Frequency Modulated Continuous Wave (FMCW) Radar. 2022. Conference Paper Publisher: IEEE. *TransNav, the International Journal on Marine Navigation and Safety of Sea Transportation*. 2009. **3** (3). P. 311–314. https://www.transnav.eu/Article_CRM-203_Type_Frequency_Modulated_Plata,11,171.html
17. Kosovets M. Generating a Test configuration with absorber 3D Tz FMCW Imager Radar. *Journal «Zvjazok»*. 2017. No. 1. P. 49–57. http://con.dut.edu.ua/index.php/communication/article/view/1440

Received 20.04.2023

Mykola Kosovets,
Chief Leading Constructor, Scientific-production enterprise “Quantor”,
https://orcid.org/0000-0001-8443-7805
quantor.nik@gmail.com

Lilia Tovstenko,
Leading Software Engineer, V.M. Glushkov Institute of Cybernetics of the NAS of Ukraine.
115lili@incyb.kiev.ua

UDC 517.9:621.325.5:621.382.049.77

Mykola Kosovets [1 *], Lilia Tovstenko [2]

Neural Network Component of Modern Information System on Mobile Platforms: LPI Cognitive Radar System

[1] Scientific-production enterprise “Quantor”, Kyiv, Ukraine
[2] V.M. Glouchkov Institute of Cybernetics of the NAS of Ukraine, Kyiv
[*] Correspondence: quantor.nik@gmail.com

The problem of building modern systems for collecting, processing and presenting information for moving platforms, characterized by the presence of a neural network with deep learning, sensors with preprocessing, systems processing and presenting information, is considered. In modern systems the physics of the processes does not change, and accordingly, the algorithm for extracting signals from under the noise doesn't change either but is supplemented by a neural network that learns in the process of processing information to perform an applied task. Implementation example shown the introduction of artificial intelligence technology for the design a cognitive radar on a moving platform facilitates the transition from adaptive systems to cognitive ones.

Keywords: artificial Intellect, deep learning, neural network, cognitive radar, multiprocessor, Frequency modulation continuous wave, Radar Cross-Section, Solid State Transmitter.

УДК 517.9:621.325.5:621.382.049.77

Микола Косовець [1*], Лілія Товстенко [2]

Нейромережевий компонент сучасної інформаційної системи на мобільних платформах: LPI когнітивна радарна система

[1] *Науково-виробниче підприємство «Квантор», Київ, Україна*
[2] *Інститут кібернетики імені В.М. Глушкова НАН України, Київ*
[*] *Листування:* quantor.nik@gmail.com

Вступ. Розглянуто проблему побудови сучасних систем збору, обробки та представлення інформації для рухомих платформ, що характеризуються наявністю нейронної мережі з глибоким навчанням, сенсорів з попередньою обробкою, систем обробки та представлення інформації. У сучасних системах фізика процесів не змінюється, а відповідно алгоритм вилучення сигналів з-під шуму також не змінюється, а доповнюється нейронною мережею, яка в процесі обробки інформації навчається виконувати прикладне завдання. Показаний приклад реалізації впровадження технології штучного інтелекту для розробки когнітивного радара на рухомій платформі полегшує перехід від адаптивних систем до когнітивних.

Мета. Основна мета – впровадження Штучного Інтелекту в сучасні радари різного призначення: медичні системи, системи моніторингу довкілля, системи безпеки, військові системи, системи розмінування, моніторинг у сільському господарстві та інші. Особливе місце займають системи на платформах, що рухаються: дрони, літаки, вертольоти та інші. Також приділено увагу побудові малополітних радарних систем, які досягаються малою потужністю випромінювання, застосуванням чутливих приймачів сигналів, особливістю кодування та режиму передачі, використання нейронних мереж із навчанням, класифікацією сигналів, обробкою радарних зображень тощо.

Взято радар сантиметрового діапазону, як найбільше вивчений, найбільш інформативний на сьогодні, здатного збирати інформацію на великих відстанях, малих габаритах, розмірів, споживання, вазі. Маючи потужність випромінювання в один *Вт,* ми можемо сканувати об'єкти на відстані 20 км. Сам процес проектування мережного приймально-передавального пристрою мало чим відрізняється від звичайного, за винятком системи управління роботою приймально-передавального тракту з рівнем сигналу нижче шумів і когнітивних можливостей. Інтерес обумовлений інформативністю та відносною простотою проектування. Вони різняться по частоті, чутливості, потужності, модуляції, кількості інформації, інтерфейсу, виявлення об'єктів тощо.

Результати. Розглянутий компонент нейронної мережі: радіохвильовий приймач та передавач сантиметрового діапазону. Спроектований сучасний радар з низькою ймовірністю перехоплення (LPI) є класом радіолокаційної системи, що має певні характеристики, які роблять їх практично невидимими для сучасних приймачів перехоплення. Особливості радарів LPI включають: використання вузькоспрямованої антени з низькими бічними пелюстками; передача радіолокаційних імпульсів лише у разі потреби; зниження потужності переданого імпульсу; поширення радіолокаційних імпульсів у широкій смузі частот, тому у будь-якій смузі буде дуже слабкий сигнал; або використовувати різні параметри передачі, такі як форма імпульсу, частота повторення імпульсів (PRF) за допомогою внутрішньоімпульсної модуляції.

Висновки. Представлена схема приймально-передавального тракту системи радіолокації сантиметрового діапазону. Він має типові блоки радіолокації прийому і передачі, опорні генератори, змішувачі, підсилювачі, циркулятор, перемикачі, обмежувачі сигналів, аналого-цифрові і цифро-аналогові перетворювачі. Ця відмінність від аналогічних радарів, де регуляція якісних характеристик досягається адаптивними методами, а шляхом регуляції когнітивних здібностей радара нейронною мережею. У цій статті представлені характеристики відбитих сигналів, вплив на них перешкод, зовнішніх і внутрішніх шумів. Це дозволить інструментам глибокого навчання створити когнітивний радар з характеристиками, які визначає Замовник.

Ключові слова: штучний інтелект, глибоке навчання, нейронна мережа, когнітивний радар, мультипроцесор, частотна модуляція безперервної хвилі, твердотільний передавач.